Importance of Deck Details in Bridge Aerodynamics

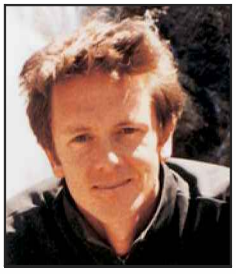

Luca Bruno
Assist. Prof.
Polytechnic of Torino
Torino, Italy

Luca Bruno, born 1971, received a degree in Architecture from Politecnico di Torino, a diploma in Structural Dynamics and Coupling Effects from ENPC in Paris, two PhD in Structural Engineering from Politecnico di Torino and in Fluid Mechanics from Université de la Méditerranée, Marseille, France. He is currently assistant professor at Politecnico di Torino.

Giuseppe Mancini
Prof.
Polytechnic of Torino
Torino, Italy

Giuseppe Mancini, born in 1947, is professor of Structural Engineering and Bridge Design at Politecnico di Torino – Italy. He is Chairman of Project Team for Eurocode 2.2, Concrete Bridge Design, and Deputy Chairman of CEN/TC 250/SC2, Concrete Structures. He is too Deputy Chairman of Steering Committee and Member of *fib* Praesidium.

Peer-reviewed by international experts and accepted for publication by IABSE Publications Committee

Paper received: January 22, 2002
Paper accepted: July 16, 2002

Summary

This paper focuses on the effects of the deck equipment – such as median dividers, edge safety barriers or parapets – on the aerodynamic response of long-span suspension and cable-stayed bridges. The importance of modelling such members in the analysis of bridge aerodynamics is demonstrated using numerical simulations both with and without barriers. The numerical technique is applied to two famous long-span bridge decks (the Normandy cable-stayed bridge and the Great Belt suspension bridge), presented by different cross section geometries and various aerodynamic characteristics. The obtained results are compared with each other and with wind-tunnel data. In particular, the numerical modelling of the barriers provides a closer insight into the mechanisms responsible for the vortex-induced oscillations of the Great Belt East bridge in 1998.

Introduction

The knowledge of wind action exerted on deck covers a prominent role in the design of long-span bridges. The analysis of the aerodynamic and aeroelastic instabilities associated with bridges has rapidly advanced since the well-known Tacoma failure in 1940 [1]. In spite of the historical progress and extensive wind tunnel tests, the large wind-induced oscillations which occurred in 1998 at the Great Belt East Bridge [2] (*Fig. 1*) confirmed that the aerodynamic analysis of the deck still remains a critical task during the design process in terms of accuracy, costs and time requirements.

The aim of this study is to increase the accuracy of the simulations by pointing out the equipment effects on the overall wind load acting on the deck. In fact, the effects of such deck members on its aerodynamics have been little studied up to now. Bienkiewicz [3] qualitatively showed the effects of traffic barriers on the aerodynamic response of a bridge deck. Adopting the same approach, Scanlan et al [4] indicated the critical dependence of flutter derivatives upon even minor details, such as deck railings. Furthermore, the same authors consider the modelling of the section details as a critical component of wind-tunnel tests. This is because of a number of difficulties:

– to single out the influence of particular features in the geometry or in the flow
– to detect and measure small-size, complex flow structures
– to respect the conditions of aerodynamic similitude of the model.

In particular, the solidity ratio of the prototype barriers cannot be reproduced in the model by a simple scaling of their dimensions [4]. The design procedures imposed by some of the more advanced national codes [5] or adopted in the case of special works generally suffer from such difficulties by showing an incomplete knowledge about the topic.

Because the equipment is so small, the perturbations induced by these members on bridge aerodynamics are expected to be mainly due to interference phenomena with the deck. Hence, such effects should be evaluated with respect to various deck shapes and to the flow pattern respectively associated. *Fig. 2* schematically shows a possible classification of the bridge decks according to their degree of bluffness [6].

Generally, a bluff body is characterised by the separation of the boundary layer, whereas such a phenomenon does not occur around a perfectly streamlined section (airfoil) at least at low incidences [7].

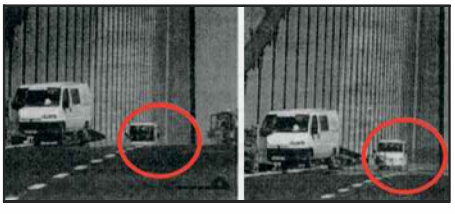

Fig. 1: Vertical oscillations of Great Belt East Bridge deck (from [2])

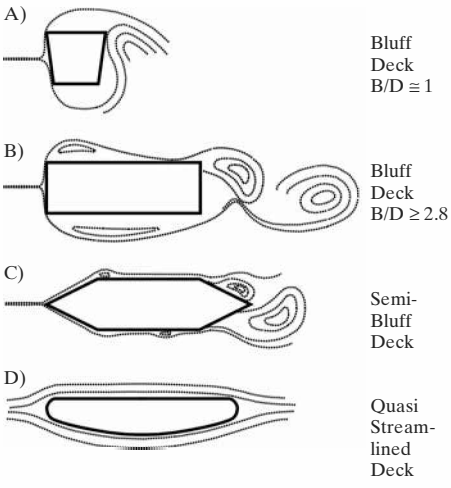

Fig. 2: Bridge deck sections with different degree of bluffness

Sections A) and B) are generally adopted for short and medium span bridges. Their shaping involves unsteady flows characterised by large vortical structures shed at the windward sharp edges. At low values of the B/D ratio, the whole section is included in the region of separation and the vortex-shedding frequency (Strouhal number $St = Df_s/U_0$) is unique, whereas for values B/D ≥ 2.8 the separated flow unsteadily reattaches along the side surfaces and discontinuities or double mode of the lift fluctuations occur. On the other hand, sections C) and D) have been extensively employed during the last decades in the field of long-span bridges. Even if it is sometimes difficult to clearly establish the borderline between such classes, the last one is generally subjected to steady aerodynamic forces. On the contrary, the semi-bluff sections are often prone to unsteady vortex-induced forces characterised by a spread frequency content. Such phenomenon is of great interest from the practical point of view. In fact, it occurs at a relatively low range of wind speeds and can markedly affect the durability and serviceability of the structure. For such reasons, the effects of the barriers are evaluated in the present study for two case studies coming from classes D (Normandy bridge) and C (Great Belt East bridge).

Numerical Prediction of Bridge Aerodynamics

The adoption of the numerical approach in this analysis permits the previously mentioned difficulties in the experimental study of the equipment effects on bridge aerodynamics to be overcome.

The detailed description of the flow modelling and of the numerical procedures adopted in the simulations overcomes the objectives of this paper. Nevertheless, it is important to remember that the direct numerical solution of the complete Navier-Stokes equations remains up to now unachieved for the high Reynolds number, turbulent flows typical of bridge aerodynamics. Despite such limitations, simplified models can actually represent a complementary approach to the aerodynamic analysis of bridge decks if they are able to describe the fundamental physical features of the problem [7]. In this study, the so-called LES (Large Eddy Simulation) and RANS (Reynolds Averaged Navier Stokes) methods are respectively applied to classes C) and D). The employed numerical tools (Fluent code) and techniques have been fully discussed, optimised and validated in [8].

Applications

To clearly identify the effects of the equipment on the aerodynamic behaviour of the bridge deck and their impact on the design process, the results of both applications are illustrated in four steps:

1) The numerical approach is briefly validated with respect to the experimental measurements. To do this, the pressure coefficient (*Cp*) distributions on the deck are compared. *Cp* is preferred to the aerodynamic coefficients because a perfect agreement in term of the latter does not assure the correct simulation of the flow, whereas the first allows to locally evaluate the accuracy of the results.
2) The local and global effects of the equipment are singled out by comparing the results obtained from models with and without barriers.
3) The observed discrepancies are justified by means of a closer insight into the physical modification induced by the barriers.
4) Finally, the simulated wind loading are compared with the ones prescribed by ENV 1991-2-4 [5].

The Normandy Bridge

The geometry of the Normandy Bridge deck [9] is characterised in *Table 1* consistently with [5]

B	B/D	α_1	φ_{side}	$A_{eff,\,med}$	A_{equip}
23.8	6.9	74°	0.37	0.38	<0.1%

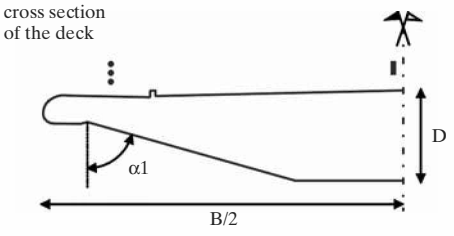

Table 1: Geometry of deck section

where the reference width B is expressed in [m], φ_{side} is the solidity ratio of the side railings

$$\varphi_{side} = \frac{A}{A_c}.$$

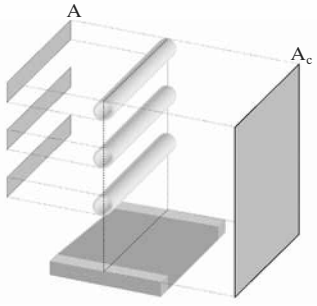

$A_{eff,\,med}$ the shadow area in elevation per meter length (effective area) of the median dividers [m²], and A_{equip} the percentage ratio between the overall cross sectional area of the barriers and the one of the box girder. *Fig. 3* shows a close-up view of the mesh adopted in the numerical simulation.

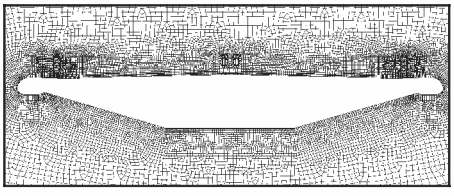

Fig. 3: Grid system near equipped cross section

Fig. 4 shows the *Cp* distributions on the deck surfaces.

The results obtained from computational models with barriers (labelled "equipped") and without barriers ("bare") are compared with those obtained in the wind tunnel tests [10] (labelled "wind tunnel data – section model"). The results obtained with the equipped deck are in good agreement with the experimental ones. The most surprising result follows from the comparison of the *Cp* distributions on the equipped and bare decks. In spite of the attention paid by the designers to reduce the wind effects on the side railings using circular profiles, the

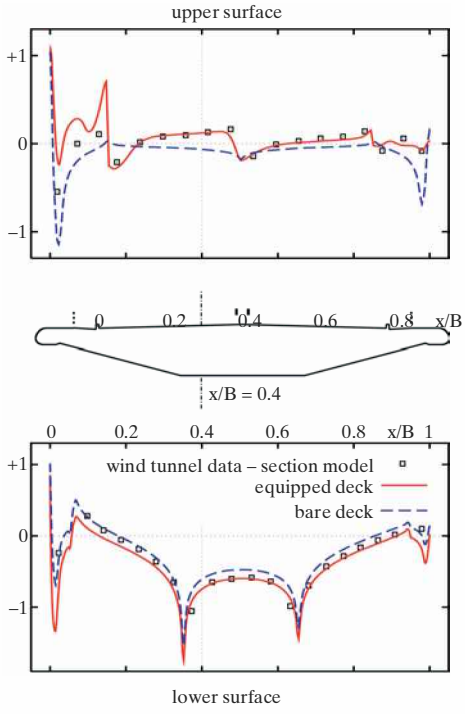

Fig. 4: Cp distributions on deck

equipment does not only locally modify the pressure field on the road surface, but also dramatically affects the *Cp* distribution on the lower surface of the deck. This global effect is not hardly surprising when looking at the physics of the flow. In fact, parapets and median dividers, even if characterised by apparently low solidity ratios, have a relevant blockage effect with respect to the flow passing over the upper surface of the girder. Then, the flow is deviated along the lower surface where its speed U_x/U_{inf} is locally increased (*Fig. 5*).

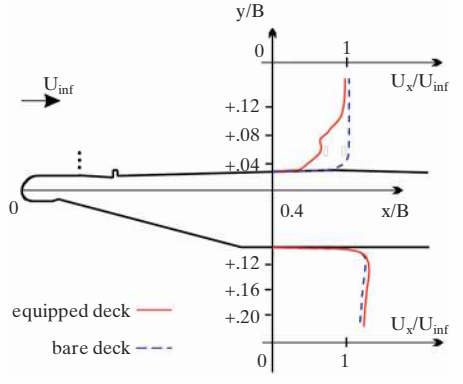

Fig. 5: Velocity profiles at x/B=0.4

Bearing in mind the well-known Bernoulli equation, the higher velocity in the equipped configuration involves a higher suction on the lower surface of the girder.

These changes in the pressure field, in addition to the ones exerted on the tangential stresses distribution, deeply modify the resultant aerodynamic force acting on the deck. The evolutions of the aerodynamic coefficients

$$C_X = \frac{2F_X}{\rho U_0^2 B}; \qquad C_Y = \frac{2F_Y}{\rho U_0^2 B}$$

expressed in the profile axes versus the angle of attack are plotted in *Fig. 6*. To single out the direct contribution of the barriers, in the equipped deck, the normal and tangential stresses have been integrated on the box girder surface ("box component") and on the overall surface of the equipment ("barriers component"). Moreover, the interference phenomena can be appreciated by comparing the box component with the values related to the bare geometry.

The direct contribution of the equipment remains fundamentally constant versus the incidence for both C_X and C_Y. This result indicates that the deck does not exert any appreciable effect on the barriers aerodynamics in the studied range of incidences.

On the one hand, the interference effects of the barriers on the deck behaviour are relevant for both forces at every angle of attack. Hence, the interference phenomena occurring between girder and equipment are "one way" effects.

The magnitudes of both C_X and C_Y are hardly affected by the barriers, but in different ways.

The direct contribution of the equipment is significant for the force in X-direction only. The most relevant differences in its value are found at positive incidences (wind from below), indicating that the interference phenomena do not vanish when the barriers are sheltered by the deck.

As the lift coefficient, it is constantly and markedly increased in magnitude ($\Delta C_Y \approx 280\%$) at every angle of attack. Hence, the aforementioned blockage effect of the railings remains relevant in the entire usual range of incidences.

To give a comparison between the available predictions of the barriers effects on the steady wind loads acting on the case-study, *Table 2* compares the computed values of the wind forces expressed in [kN]/[m] with the ones obtained by applying ENV1991-2-4 [5] (incoming wind speed $U_0 = 44$ ms^{-1}, incidence $\alpha = 0°$).

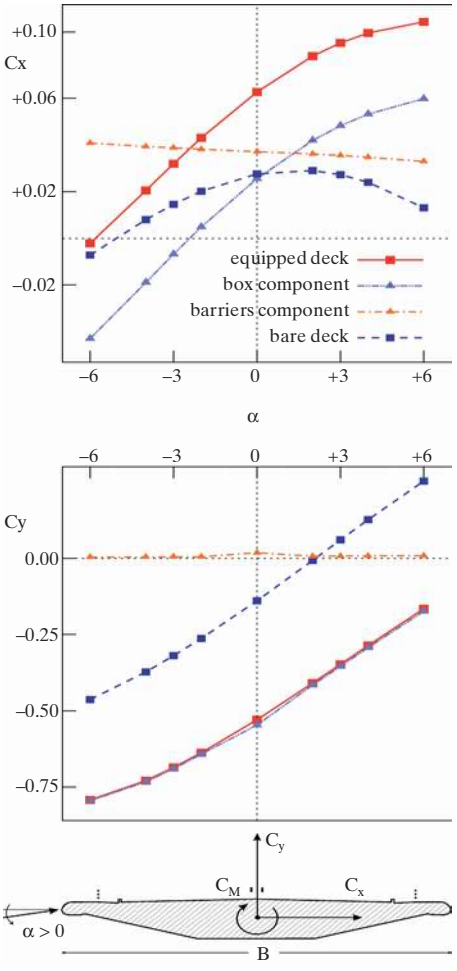

Fig. 6: Effects of deck equipment on aerodynamic coefficients

	$F_{x\,bare}$	$F_{x\,equip}$	$\Delta F_{x\,equip}$
ENV 1991-2-4	+3.80	+3.43	–9.7%
actual study	+0.79	+1.80	+127%
	$F_{y\,bare}$	$F_{y\,equip}$	$\Delta F_{y\,equip}$
ENV 1991-2-4	–12.7	–12.7	0%
actual study	–4.0	–15.2	–280%

Table 2: Wind loads on deck

The code recognises the influence of the barriers on the horizontal force only. Surprisingly, its magnitude is reduced whereas the numerical simulations indicate its relevant growth. The equipment effects on the lift force are completely neglected by the code. This is not surprising because such complex interference is hardly predictable by semi-empirical formulas.

The Great Belt East Bridge

The effects of the barriers on the steady aerodynamic forces acting on fully streamlined decks designed according to the "inversed airfoil" concept have been illustrated by means of the previous case study. On the one hand, the analysis of the equipped deck of the Great Belt East Bridge highlights

the possible effects of the equipment on the vortex-induced excitation. The final cross section of the deck [11] is described in *Table 3*.

B	B/D	α_1	φ_{side}	$A_{eff,\ med}$	A_{equip}
31	7.0	63°	0.23	0.16	<0.07%

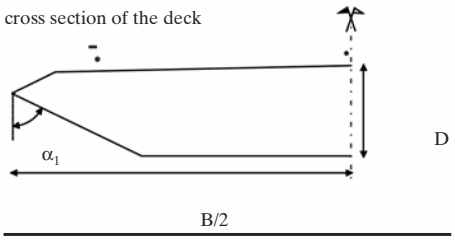

Table 3: Geometry of deck section

It is important to outline that the B/D ratio (one of the main geometrical parameters characterising the aerodynamic behaviour of the deck according to [5]) is the same as that of the Normandy Bridge. On the one hand, the safety barriers used are more porous than the ones adopted for the previous case study. The computational grid adopted around the equipped deck is shown in *Fig. 7*.

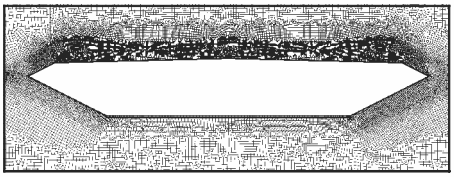

Fig. 7: Grid system around deck

A preliminary numerical study was undertaken to identify the vortex-shedding mechanism around the deck. In fact, the unsteady motions of vortical structures around the deck and in its wake play an important role in the production of aerodynamic forces, in terms of their mean value and frequency content. *Fig. 8* schematically illustrates the flow pattern around the deck by means of the computed instantaneous streamlines.

The instants t_1 and t_2 respectively correspond to a local maximum and minimum value of the lift force. The main vortical structures around the deck are located at its lower surface and in the near wake. The vortices v_1, developing from the separation bubble downstream at the lower windward corner, travel across the intrados. Independently, another eddy (v_2) is emerging in the near wake region close to the lower side panel. When the advected vortices v_1 pass the lower leeward corner they coalesce with the vortex v_2 and shed in the wake.

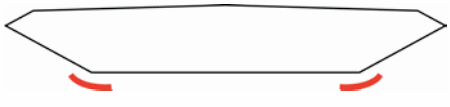

Fig. 8: Vortex shedding process around Great Belt East Bridge deck

The two vortex-shedding mechanisms described here explain the spread frequency content of the lift force experimentally measured ($0.109 \le St \le 0.158$) [12].

This description of the shedding process justifies the effectiveness of the guide vanes installed as an add-on retrofit measure [2] to mitigate the unacceptable vortex-induced oscillations (r.m.s. resonant amplitudes y_{max} = 0.25m, r.m.s. acceleration level $\ddot{a} \approx 0.03g$ [13]) related to the 5th mode (natural frequency n_e = 0.205 Hz) which occurred after the bridge completion (*Fig. 9*). In particular, the positioning of such vanes, first designed at the bottom/side panel joints to be effective in case of traffic queues [11], is justified by avoiding the merging between vortices travelling along the intrados. Once the vortex formation process has been clarified, it is possible to establish the role played by the equipment.

It is important to schematically distinguish local phenomena (that is, the ones concerning the neighbourhood of the equipment) and global effects. Two local interference effects of the barriers are clearly visible in *Fig. 8*.

First, the separated shear layer at the upper surface is reattached thus avoiding a larger separation bubble. In addition to observing the excellent agreement of the numerical simulations with the experimental measurements [12], the analysis of the distributions of the mean pressure coefficient and of its standard deviation on the deck (*Fig. 10*) permits the appreciation of the effects of the flow reattachment on the pressure field. The windward side railing acts as a guide vane maintaining the flow attached to the intrados downstream the leading upper-side panel. Hence, it reduces both the mean value of the suction and the pressure fluctuations on the windward traffic lanes ($0.06<x/B<0.5$). Once more, the effectiveness of the railings grows at positive incidences (α = + 6°). This phenomenon, in addition to the higher suction at the lower surface due to the aforementioned blockage effect of the rails, determines the lower mean value of the force in Y-direction acting on the equipped deck at positive incidences (*Fig. 11*). The effect of the barriers on the mean aerodynamic forces is reduced with respect to the case

	$F_{x\ bare}$	$F_{x\ equip}$	$\Delta F_{x\ equip}$
ENV 1991-2-4	+4.84	+4.23	–12.6%
actual study	+2.59	+3.24	+25.1%
	$F_{y\ bare}$	$F_{y\ equip}$	$\Delta F_{y\ equip}$
ENV 1991-2-4	–16.1	–16.1	0%
actual study	–6.8	–7.5	–9.5%

Table 4: Wind loads on deck (U_0 = 44 ms^{-1}; α = 0°)

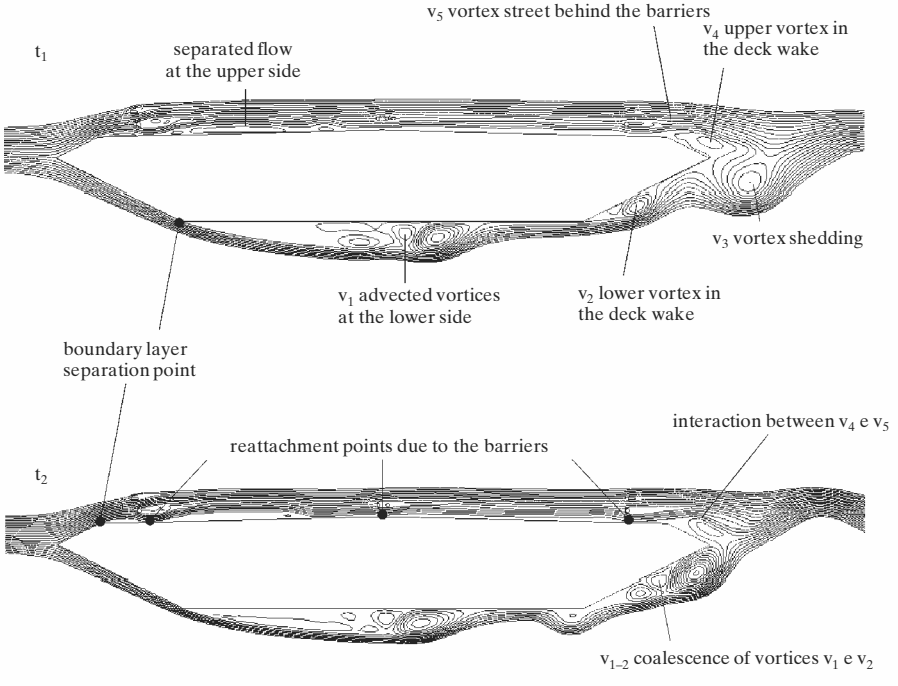

Fig. 9: Guide vanes for suppression of vortex-induced response

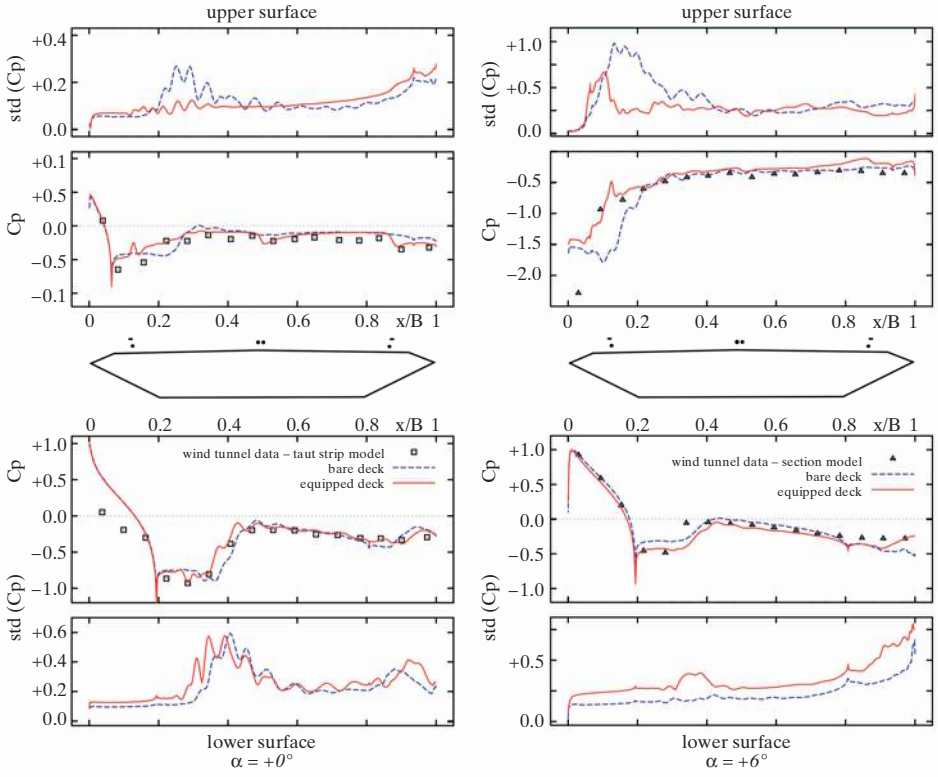

Fig. 10: Effects of the barriers on Cp distributions at two incidences

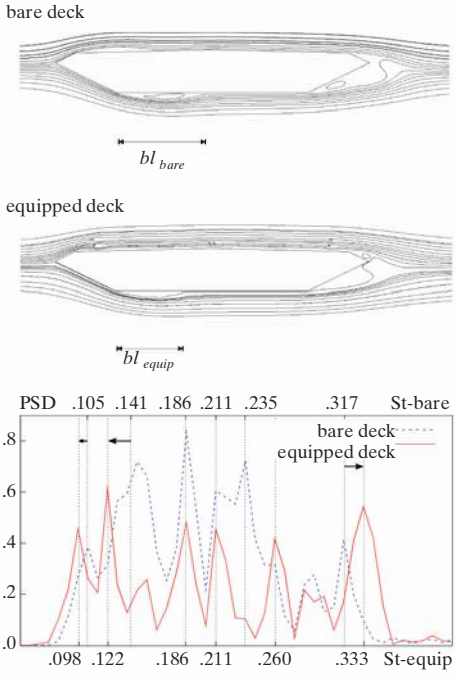

Fig. 13: Mean streamlines and frequency content of lift force

study of the Normandy Bridge (*Tables 2* and *4*).

This is certainly due to the reduced porosity ratio of the side rails (*Tables 1* and *3*), but also to the disturbed separated flow in which they are positioned. Owing to this feature, the increment of the drag force cannot

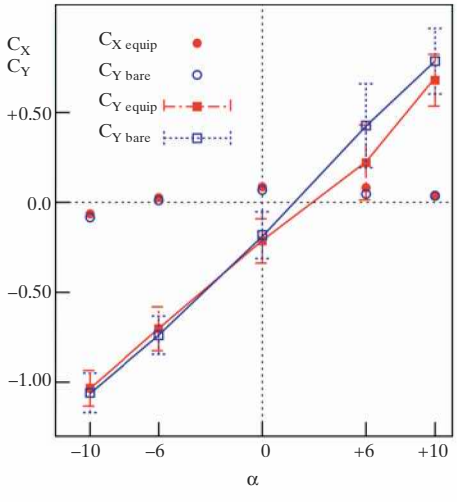

Fig. 11: Effects of barriers on aerodynamic coefficients

be completely related with the direct contribution given by the barriers. Hence, attention is focused on the contribution of the near wake (base) region of the deck.

Fig. 12 shows the mean velocity defect along two straight lines at different locations in the wake. The barriers increase the ratio between the width of the wake and that of the deck. Hence, the distance between vortices of different signs increases and the deck experiences a higher value of drag force. The second local phenomenon is induced by the leeward side railings and impacts the vortex shedding mecha-

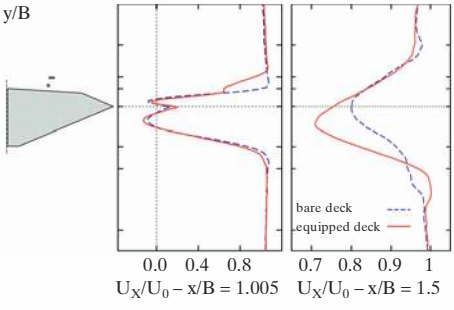

Fig. 12: Velocity defect in wake

nisms. As depicted in *Fig. 8*, small eddies (v_5) are shed in a classical Karman street downstream the circular side railings.

This high frequency vortex-shedding is probably responsible for the higher frequency content of the lift force in the equipped configuration (upper bound of the Strouhal range from 0.317 to 0.333 (*Fig. 13*).

On the other hand, the vorticity of these eddies is mixed with one of the adjacent eddies v_4 and quickly disappears along the wake (*Fig. 12*). Owing to the high frequency content and the moderate level of energy, the fluctuating force induced by the vortex-shedding has no relevant effects on the structural response of the bridge. But surprisingly, the barriers also affect the lower bound of the Strouhal numbers range, that is, the shedding frequency related to the interaction between the vortices v_1 shed from the separation bubble and the vortices v_2 that emerge past the leeward edge. Once more, this effect is due to the blockage effect of the barriers. Because of this, the velocity increases along the lower side of the deck with respect to the bare geometry. As the velocity outside the outer boundary layer at the separation point increases, the instantaneous flux of vorticity also increases. Then, the vorticity shed downstream the separation bubble is higher and more concentrated. Consequently, the vorticity, convected along the lower surface of the deck, moves downstream the maximum velocity defect in the wake (*Fig. 12*). The more concentrated vorticity reduces the length of the separation bubble and permits to correctly predict the experimental pressure distribution (*Fig. 10*) $\alpha = +0°$, $0.2<x/B<0.4$). As a result, of the reduction in length of the bubble bl_{equip} (*Fig. 13*), the vortices v_1 cover a longer length to reach the leeward edge and to merge into the vortices v_2. Hence, the shedding period becomes longer and the associated Strouhal number (*Fig. 13*) is reduced from $0.105 \le St \le 0.141$ (without barriers) to $0.098 \le St \le 0.122$ (with barriers, $\Delta St_{equip} \approx -8.5\%$).

In ENV 1991-2-4 [5] a semi-empirical formula is suggested for predicting an unique Strouhal number for bridge decks

$$St = \left(1.1\frac{B}{D} + 1\right)^{-1} = 0.114 \quad \text{for } 5 \le \frac{B}{D} \le 10$$

The predicted value is in good accordance with both the equipped numerical simulation and experimental measurements (1:80 model with barriers). However, such agreement seems to be due to an accidental case taking into account that any parameter related to the equipment appears in the formula so that their influence is completely neglected.

The reduction of the Strouhal number induced by the barriers is, according to the authors, of primary importance with respect to the resonant conditions. *Table 5* summarizes the ratio between the frequency of vortex shedding f_s and the natural frequency n_e and the critical wind velocity u_{crit} for the 5th and 8th mode of cross-wind vibration.

mode	f_s/n_e		u_{crit}	
	bare	equip	bare	equip
5th	1.09	1.00	7.3	8.0
8th	0.57	0.52	14.0	15.3

Table 5: Resonant vortex-shedding conditions

Firstly, the numerical simulations clearly indicate that in the case study the blockage effect of the barriers approaches the resonant condition for the 5th mode. The corresponding critical wind speed is in good accordance with the full-scale measurements [13].

Secondly, the obtained results could contribute to explain some of the uncertainties encountered in the wind-tunnel tests during the design of the bridge. In fact, the wind-tunnel test carried on the section model (scale 1:80) [12] indicated the excitation of the 5th mode (r.s.m. y_{max} = 0.30m), well simulating the full-scale behaviour. On the contrary, the full-aeroelastic bridge model (scale 1:200) [11] underestimated the maximum amplitudes (r.s.m. y_{max} = 0.13m) related to the 8th mode (n_e = 0.39 Hz). Due to this uncertainty, the bridge was only prepared for guide vanes during the design phase and their installation was kept in reserve according to a "wait and see" strategy. As the model scale becomes smaller, the aerodynamic similitude of the barriers is corrupted and their effective porosity decreases. Hence, the blockage effect of the equipment increases and the lower Strouhal number is underestimated. In such a way the small-scale full-aeroelastic model, even if it accurately simulates the 3-dimensional dynamic characteristics of suspended structures, could erroneously predict the frequency content of the vortex-shedding excitation and thus the dynamic response of the bridge.

Conclusions

In this paper, the authors have attempted to discuss the role played by the equipment on the aerodynamic behaviour of long-span bridge decks.

Firstly, the authors tried to shed new light on the essential physical features of the complex aerodynamic interferences occurring between the deck and its equipment. The numerical simulations demonstrated their aptitude to contribute to the understanding of the physics of the flow, allowing information to be obtained that could not have been derived from experiments.

Secondly, the effects of these fluid flow phenomena on the steady and fluctuating wind loads acting on the deck are singled out. From comparison made between the simulated forces and the ones predicted by ENV 1991-2-4 follows that standards rules generally give inadequate design guidance and incorrect results in the case of decks with complex geometries (errors up to 200%). To partially fill in the gaps of the more advanced codes about wind actions on bridges, the authors suggest some qualitative guidelines to be considered during concept design:

- the barriers increase the overall degree of bluffness of the section
- as the barriers solidity ratio becomes larger, the its effect are more relevant. A value of $\varphi_{side} \approx 30\%$ should be considered very high
- as the bare deck shape is more streamlined, the effects are more relevant
- the main effects of the equipment on the mean values of the aerodynamic forces can be summarised in: a) the rise of the drag force; b) the lowering of the mean value of the lift force
- in the case of semi-bluff sections prone to vortex shedding, further effects can be outlined: c) the reduction of the amplitude of the lift fluctuations; d) the redistribution of the lift frequency content in a broader band.

In the later design phases – and especially in the case of flexible bridge structures – the numerical simulation represents a useful complementary method of analysis of the aerodynamic behaviour of the actual deck section. In spite of the increased computational effort, the numerical modelling of the barriers is strongly recommended to take into account correctly their features and their global effects on the flow.

References

[1] LARSEN, A. *Aerodynamics of the Tacoma Narrows Bridge – 60 years later,* Structural Engineering International, 4, 2000, IABSE, Zurich, pp. 243–248.

[2] LARSEN, A.; ESDHAL, S.; ANDERSEN, J.E.; VERJUM, T. *Vortex shedding excitation of the Great Belt suspension bridge.* Proc. 10th International Conference on Wind Engineering. Balkema, Rotterdam, 1999, pp. 947–954.

[3] BIENKIEWICZ, B. *Wind tunnel study of geometry modification on aerodynamics of a cable-stayed bridge deck.* J. Wind Eng. Ind. Aerodyn., 26, 1987, pp. 325–339.

[4] SCANLAN, R.H.; JONES, N.P.; SARKAR, P.P.; SINGH, L. *The effect of section model on aeroelastic parameters,* J. Wind Eng. Ind. Aerodyn., 54-55, 1995, pp. 45–53.

[5] CEN, ENV 1991-2-4 – *Wind Actions on Bridges, Brussels,* 1995.

[6] SHIRAISHI N.; MATSUMOTO M. *On classification of vortex-induced oscillation and its application for bridge structures.* J. Wind Eng. Ind. Aerodyn., 14, 1983, pp. 419–430.

[7] BURESTI, G. *Vortex shedding from bluff bodies,* Proc. Wind Effects on Buildings and Structures, Rotterdam, 1998, pp. 61–95.

[8] BRUNO, L. *Aerodynamic behaviour of long-span bridge decks* (in Italian), PhD thesis in Structural Engineering (Politecnico di Torino) and in Fluid Mechanics (Université de la Méditerranée – Aix-Marseille II), 2001.

[9] VIRLOGEUX, M. *Wind design and analysis for the Normandy bridge,* Proc. First International Symposium on Aerodynamics of Large Bridges. Balkema, Rotterdam, 1992, pp. 183–216.

[10] SZECHENYI, E. *Pont de Normandie: effets du vent; étude aéroélastique – essais.* Rapport interne 10/3588 RY070R370G, ONERA, Paris, 1987.

[11] LARSEN, A. *Aerodynamic aspects of the final design of the 1624 m suspension bridge across the Great Belt.* J. Wind Eng. Ind. Aerodyn., 48, 1993, pp. 261–285.

[12] REINHOLD, T.A.; BRINCH, M.; DAMSGAARD, A. *Wind-tunnel tests for the Great Belt Link.* Proc. Int. Symp. on Aerodynamics of Large Bridges, Balkema, Rotterdam, 1992, pp. 255–268.

[13] FRANDSEN, J.B. *Simultaneous pressures and accelerations measured full-scale on the Great Belt East suspension bridge.* J. Wind Eng. Ind. Aerodyn., 89(1), 2001, pp. 95–129.